



## Analytical Model for Hook Anchor Pull-Out

Brincker, Rune; Ulfkjær, J. P.; Adamsen, P.; Langvad, L.; Toft, R.

*Published in:*

Modern Design of Concrete Structures : Proceedings of Nordic Symposium, Aalborg University, May 3-5, 1995

*Publication date:*  
1995

*Document Version*  
Acceperet manuscript, peer-review version

[Link to publication from Aalborg University](#)

*Citation for published version (APA):*

Brincker, R., Ulfkjær, J. P., Adamsen, P., Langvad, L., & Toft, R. (1995). Analytical Model for Hook Anchor Pull-Out. I Aakjær, K. (ed.) (red.), *Modern Design of Concrete Structures : Proceedings of Nordic Symposium, Aalborg University, May 3-5, 1995: R / Institut for Bygningsteknik, Aalborg Universitet* (R9513 udg., s. 47-62). Dept. of Building Technology and Structural Engineering, Aalborg University. The Nordic Symposium on Modern Design of Concrete Structures Nr. R9513

### General rights

Copyright and moral rights for the publications made accessible in the public portal are retained by the authors and/or other copyright owners and it is a condition of accessing publications that users recognise and abide by the legal requirements associated with these rights.

- Users may download and print one copy of any publication from the public portal for the purpose of private study or research.
- You may not further distribute the material or use it for any profit-making activity or commercial gain
- You may freely distribute the URL identifying the publication in the public portal -

### Take down policy

If you believe that this document breaches copyright please contact us at [vbn@aub.aau.dk](mailto:vbn@aub.aau.dk) providing details, and we will remove access to the work immediately and investigate your claim.

## ANALYTICAL MODEL FOR HOOK ANCHOR PULL-OUT

Rune Brincker, Associate Professor of Civil Engineering  
Jens Peder Ulfkjær, Assistant Professor of Civil Engineering  
Peter Adamsen, M.Sc.  
Lotte Langvad, M.Sc.  
Rune Toft, M.Sc.  
University of Aalborg

### Abstract

A simple analytical model for the pull-out of a hook anchor is presented. The model is based on a simplified version of the fictitious crack model. It is assumed that the fracture process is the pull-off of a cone shaped concrete part, simplifying the problem by assuming pure rigid body motions allowing elastic deformations only in a layer between the pull-out cone and the concrete base. The derived model is in good agreement with experimental results, it predicts size effects and the model parameters found by calibration of the model on experimental data are in good agreement with what should be expected. Keywords: hook anchor, analytical model, fracture mechanics, fictitious crack model.

### Introduction

Anchors are used in most reinforced concrete structures. It might be simple adhesive anchors, expansion anchors or hook anchors, figure 1. Usually, the simple adhesive anchor, figure 1.a is used where it is possible. It is simple and reliable. Further, since this anchor is usually designed in such a way that the load bearing capacity of the adhesive anchor relies on the shear resistance of the interface between the bar and the concrete, the failure process is ductile, and thus, as for all ductile failure problems, no or at least small size effects are observed.

However, the simple adhesion anchor needs a relatively long embedment length to ensure enough load-bearing capacity, and to ensure that the failure of the anchor will be pull-out of the anchor bar. If the space is limited and the embedment length is reduced, there is a risk that the mode of failure will change from pull-out of the bar to pull-off of a concrete cone. In this case, the failure is more brittle, and the load-bearing capacity no longer depends on the shear resistance of the interface. In this case, the load-bearing capacity depends on the fracture energy of concrete material and of the size and the shape of the pulled-off concrete cone. The bigger the cone, the larger the load-bearing capacity, and, thus, it is natural to force the concrete cone to start as deeply as possible. This can be done by introducing an expansion part at the end of the anchor, figure 1.b, but the safest

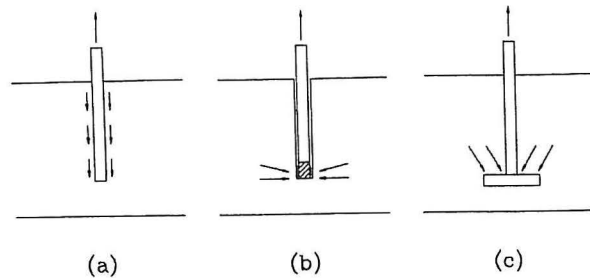


Figure 1. Different ways of transferring the load from the anchor bolt to the concrete, a) adhesive anchor, b) expansion anchor and c) hook anchor.

way of ensuring the cone to start at the end of the anchor is to provide the anchor with a "hook", usually shaped like an anchor plate at the end of the anchor bar, figure 1.c.

As already mentioned, since the failure of the hook anchor mostly depends on the fracture mechanical properties of the concrete, the load-bearing capacity is expected to show a clear size effect. These size effects have been observed by several researchers, Bocca et al. [1], and by Eligehausen and Savade [2]. Their results indicate a strong size effect over embedment depth ranging from 50 mm to 500 mm.

Eligehausen and Clausnitzer [3] studied the behaviour of anchors by finite element models. Their investigation showed a clear influence of the type of model used. A ideal plastic model gave higher load-bearing capacities than a more brittle model using material softening.

Elfgren et al. [4] also studied the problem numerically using a fictitious crack model approach for the softening material. Their investigation indicates, that the shear stresses in the crack should be incorporated in the model. Also Rots [5] investigated the problem numerically. He studied the influence of the number of radial cracks (cracking of the concrete cone) and used a smeared crack approach. His results indicate that the number of radial cracks tend to increase the ultimate load. Elfgren and Ohlson [6] studied the influence of tensile strength and fracture energy using a finite element analysis. As expected, their results indicate that the ultimate load and the ductility of the failure process increase with the fracture energy, and that increasing the tensile strength will increase the ultimate load and the brittleness of the failure process.

Bocca et al. [1] made an analysis using the fictitious crack model in a finite element analysis using axi-symmetric elements and a re-meshing technique. They found good agreement with experimental results. Also Ozbolt and Eligehausen [7] made a finite element analysis using axi-symmetric elements. They showed that cracking starts at about 30 % of the ultimate load, and that the ultimate load is mainly determined by the fracture energy. Also, their results indicate a strong size effect on the ultimate load.

Tommaso et al. [8] investigated the influence of the shape of the crack opening relation. They found that a bi-linear softening curve predicts more realistic results than a single-linear curve. Similar results have been found by Urchida et al. [9]

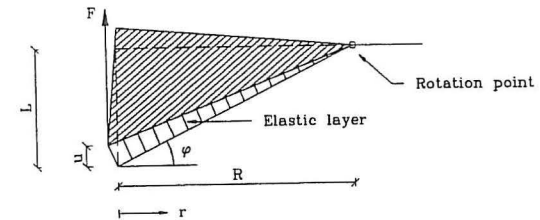


Figure 2. Geometry of simplified fictitious crack model.

### Basic assumptions

In this section the basic assumptions of the simplified models describing anchorage pull-out using the fictitious crack approach is presented.

The fictitious crack model is due to Hillerborg [10], but the basic idea is close to that of Dugdale, [11] who used a similar approach assuming a constant yield stress in the fracture zone, and Barenblatt [12], who assumed a more general distribution of the stresses in the fracture zone. Usually the fictitious crack model concept is used in finite element programs using special no-volume elements [13] or using the smeared crack approach [14], or it might be formulated using sub-elements describing the elastic behaviour and introducing the softening only for the material in the a pre-selected crack path, Petersson [15], Brincker and Dahl [16]. However, these methods are complicated and time-consuming to use for design, and they do not provide simple analytical solutions indicating the degree of brittleness and indicating how strongly a certain problem might be influenced by size effects. Thus, it is desirable to have simple models that describe the basic fracture behaviour qualitatively correct in order to have simple tools especially for describing the brittleness of the failure process.

The intention of the models presented here is to formulate the simplest possible model that reflects the basic fracture mechanical behaviour. The model problem is illustrated in figure 2. The problem is assumed to be plane, i.e. the 3-dimensional problem is not considered, and thus radial crack are omitted from the analysis. Further, the crack path is assumed to be linear, the slope being described by the angle  $\varphi$ , and the deformation is assumed to be a rigid body motion as a rotation around the point where the crack path meets the surface of the concrete. The depth  $L$  is related to the radius of the cone by the equation  $L = R \tan(\varphi)$ . The cone and the surrounding concrete is assumed to be perfectly rigid, all the elasticity being described by an elastic layer between the cone and the rest of the body. This simple approach has proved its value in modelling of the failure process for unreinforced and reinforced beams, Ulfkjær et al. [17-19].

In the distance  $r$  from the edge of the anchor stud the vertical deformation  $w$  is

$$w = u(1 - \frac{r}{R}) \quad (1)$$

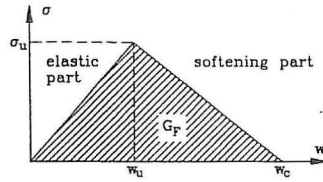


Figure 3. Stress-deformation relationship for the case of single-linear softening.

This deformation will cause vertical as well as horizontal stresses in the elastic layer, and horizontal as well as vertical reactions at the rotation point. However, in this simplified analysis, it will be assumed, that the geometry is chosen in such a way, that the vertical reactions at the rotation point can be neglected. Thus, considering only vertical stresses  $\sigma = \sigma(r)$ , the corresponding force is given by

$$F = \int_0^R 2\pi r \sigma(r) dr \quad (2)$$

### Single-linear softening

For the case of single-linear softening the physical relation of the layer is as shown in figure 3, i.e. the elastic part is linear and the softening part is linear. Here  $w$  is the total deformation and, thus, it includes elastic as well as softening terms.

For any point in the crack path, as long as the stresses have not reached the ultimate stress  $\sigma_u$ , the response is linear, and no crack is present at that point. The deformation  $w_u$  where the softening starts is given by

$$w_u = \frac{\delta \sigma_u}{E} \quad (3)$$

where  $E$  is Young's modulus of the concrete, and  $\delta$  is the thickness of the elastic layer. eq. (3) defines the layer thickness  $\delta$ .

The fracture energy is the area below the stress-deformation relation in figure 3, i.e. the fracture energy is

$$G_F = \frac{1}{2} w_c \sigma_u \quad (4)$$

Using the introduced physical relation for the elastic layer the stress is given by

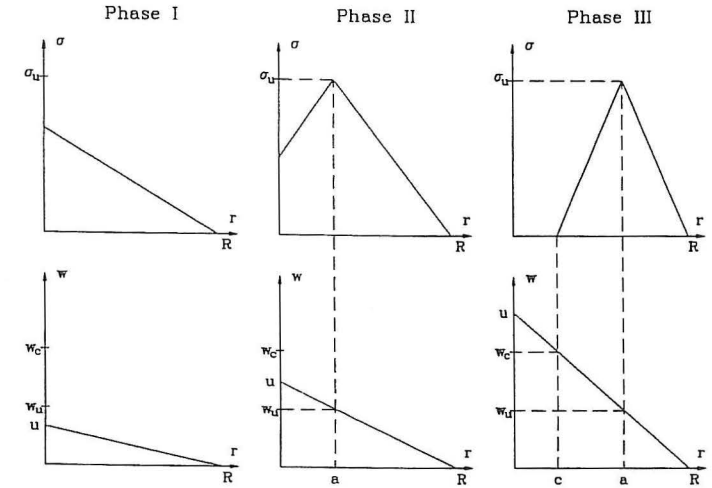


Figure 4. Stress distributions for the three phases of crack formation for the case of single-linear softening.

$$\sigma(r) = \begin{cases} w(r) \frac{\sigma_u}{w_u} & \text{for } w(r) \leq w_u \\ \sigma_u \left(1 - \frac{w(r) - w_u}{w_c - w_u}\right) & \text{for } w_u \leq w(r) \leq w_c \\ 0 & \text{for } w_c \leq w(r) \end{cases} \quad (5)$$

As it appears, this divides the fracture process into three phases. In phase I the deformation  $u$  has not reached the deformation  $w_u$  and thus, no fictitious crack is present. In phase II  $u$  is between  $w_u$  and  $w_c$ , i.e. a fictitious crack has developed. Finally, in phase III  $u$  has exceeded the critical crack opening  $w_c$  and a real crack has developed. The stress distributions for the three phases are illustrated in figure 4. Let  $c$  denote the length of the real crack, and let  $a$  denote the total length of the crack (real crack + fictitious crack). Now, using eq. (1) and (2) together with eq. (5) and carrying out the integrations, the following expression is obtained for the force

$$F = 2\pi \sigma_u \left( \frac{1}{2} (a^2 - c^2) \left(1 - \frac{u - w_u}{w_c - w_u}\right) + \frac{1}{3} (a^3 - c^3) \frac{u}{R(w_c - w_u)} \right) + 2\pi \frac{\sigma_u}{w_u} u \left( \frac{1}{6} R^2 + a^2 \left( \frac{a}{3R} - \frac{1}{2} \right) \right) \quad (6)$$

where the crack parameters  $a$  and  $c$  are given by

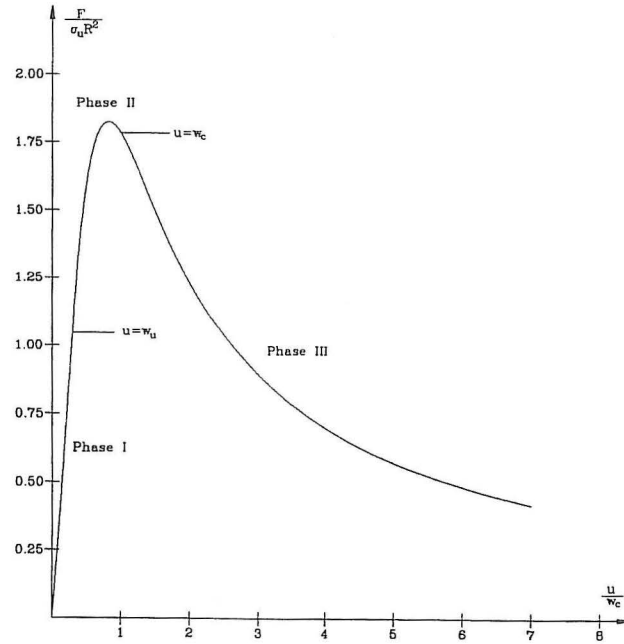


Figure 5. Relationship between force and deformation simulated by the model using single-linear softening.

$$a = \begin{cases} 0 & \text{for } u < w_u \\ R(1 - w_u/u) & \text{for } u \geq w_u \end{cases} \quad (7)$$

$$c = \begin{cases} 0 & \text{for } u < w_c \\ R(1 - w_c/u) & \text{for } u \geq w_c \end{cases} \quad (8)$$

The equations (6), (7) and (8) describe the pull-out of the concrete cone using the displacement  $u$  as the controlling parameter. To use the model the constitutive parameters  $\sigma_u$ ,  $w_u$  and  $w_c$  must be known as well as the radius  $R$  of the cone at the concrete surface. Figure 5 shows a typical load-displacement curve simulated by the model using the values  $R = 1000w_c$ ,  $w_u = \frac{2}{17}w_c$  and  $G_F = 178\sigma_u/w_c$ . The plot was made non-dimensional by dividing the force  $F$  by  $\sigma_u R^2$  and the displacements  $u$  by  $w_c$ .

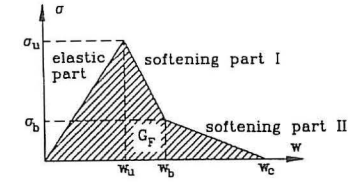


Figure 6. Stress-deformation relationship for the case of bilinear softening.

### Bilinear softening

For the bilinear softening the relationship between the vertical stress  $\sigma$  and the vertical deformation  $w$  is modelled as shown in figure 6, i.e. the softening part is modelled by a bilinear curve. This defines two new parameters describing the kink point  $\sigma_b$  and  $w_b$ .

As before, the fracture energy is easily expressed by the constitutive parameters

$$G_F = \frac{1}{2}(\sigma_u w_b + \sigma_b(w_c - w_u)) \quad (9)$$

and the vertical stresses are found as

$$\sigma(r) = \begin{cases} w(r) \frac{\sigma_u}{w_u} & \text{for } w(r) \leq w_u \\ \sigma_u + (\sigma_b - \sigma_u) \left( \frac{w(r) - w_u}{w_b - w_u} \right) & \text{for } w_u \leq w(r) \leq w_b \\ \sigma_u \left( 1 - \frac{w(r) - w_u}{w_c - w_u} \right) & \text{for } w_b \leq w(r) \leq w_c \\ 0 & \text{for } w_c \leq w(r) \end{cases} \quad (10)$$

Again the introduced cases divide the fracture process into phases. Now, instead of three cases as for the linear softening curve, four phases are introduced. The stress distribution for the last three phases are illustrated in figure 7.

As before let  $c$  denote the length of the real crack, and let  $a$  denote the total length of the crack. Now, introducing a new crack parameter  $b$  describing the point in the fracture zone corresponding to the kink point on the softening curve, figure 7, the force is obtained by using eq. (1) and (2) together with eq. (10)

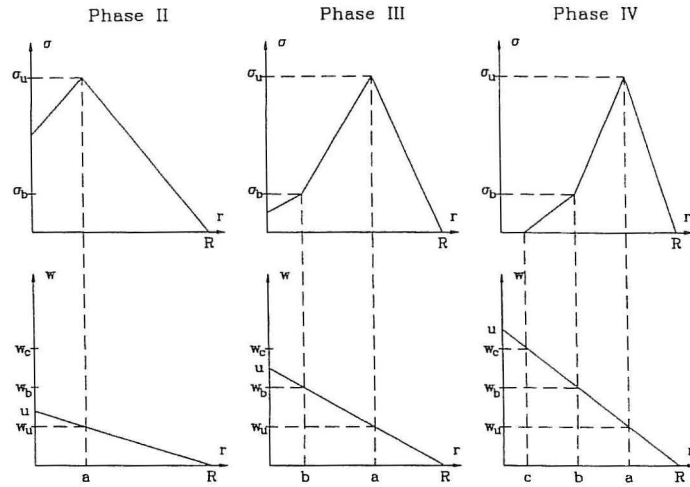


Figure 7. Stress distribution for the last three phases of crack formation for the case of bilinear softening.

$$\begin{aligned}
 F = & 2\pi\sigma_b \left( \frac{1}{2}(b^2 - c^2) \left( 1 - \frac{u - w_b}{w_c - w_b} \right) + \frac{1}{3}(b^3 - c^3) \frac{u}{R(w_c - w_b)} \right) + \\
 & + 2\pi \left( \frac{1}{2}(a^2 - b^2) \left( \sigma_u - \frac{\sigma_b - \sigma_u}{w_b - w_u} (u - w_u) \right) + \frac{1}{3}(a^3 - b^3) \frac{u(\sigma_b - \sigma_u)}{R(w_b - w_u)} \right) + \\
 & + 2\pi \frac{\sigma_u}{w_u} u \left( \frac{1}{6}R^2 + a^2 \left( \frac{a}{3R} - \frac{1}{2} \right) \right)
 \end{aligned} \quad (11)$$

where the  $a$  and  $c$  are given by eq. (7) and (8) and where

$$b = \begin{cases} 0 & \text{for } u < w_b \\ R(1 - w_b/u) & \text{for } u \geq w_b \end{cases} \quad (12)$$

For this model the constitutive parameters  $\sigma_u$ ,  $w_u$ ,  $\sigma_b$ ,  $w_b$  and  $w_c$  must be known. Figure 8 shows a typical load-displacement curve simulated by the model using the values  $R = 1000w_c$ ,  $w_u = \frac{1}{15}w_c$ ,  $w_b = \frac{1}{3}w_c$ ,  $\sigma_b = \frac{1}{4}\sigma_u$  and  $G_F = 178\sigma_u/w_c$ , and again the plot was made non-dimensional by dividing the force  $F$  by  $\sigma_u R^2$  and the displacements  $u$  by  $w_c$ .

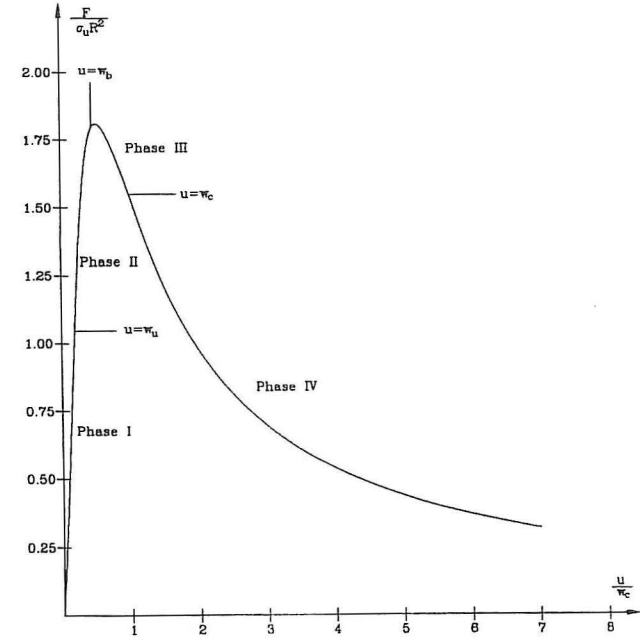


Figure 8. Relationship between force and deformation simulated by the model using bilinear softening.

### Brittleness and size effects

The introduced analytical models provide a simple way of expressing the brittleness of the pull-out problem. The classical brittleness number  $B = f_t^2 l / EG_F$ , Bache [20] might be derived from the single-linear model of the fracture of a bar in uniaxial tension using the definition

$$B = 2 \frac{w_u}{w_c} \quad (13)$$

using this definition together with eqs. (3) and (4) yields the following expressions for the brittleness number for the pull-out problem

$$B = \frac{w_u \sigma_u}{G_F} = \frac{\delta \sigma_u^2}{EG_F} \quad (14)$$

In this expression it would be natural to assume that the ultimate stress  $\sigma_u$  is proportional to the tensile strength  $f_t$  of the concrete. The thickness  $\delta$  of the elastic layer might be estimated from the initial slope  $S$  of the relation between

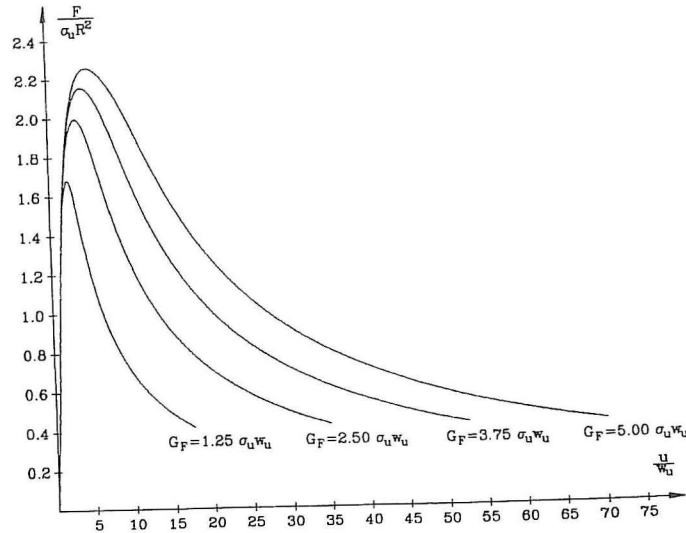


Figure 9. Influence of the brittleness number  $B$  illustrated by varying the fracture energy  $G_F$ .

the force  $F$  and the displacement  $u$  at the bottom plate. From the elastic regime of eq. (6) or (11) the relation is found as  $\delta = \frac{\pi}{3} R^2 E/S$ . The shape of the pull-out relation depends on the brittleness number  $B$ . This effect is illustrated in figure 9 showing results for the single-linear case.

Also, the shape of the softening part of the constitutive condition for the elastic layer influences the shape of the pull-out relation. This effect might be described by introducing the shape in the brittleness number  $B$ . Adopting the same definition (14) of  $B$  for the bilinear case, and limiting the bilinear softening relations to cases where the kink point of the bilinear softening path is on the same straight line as illustrated in figure 10, the shape of the softening path might be described by a single parameter

$$\beta = \frac{\sigma_b}{\sigma_u} = \frac{w_b - w_u}{w_c - w_u} \quad (15)$$

Now, introducing the fracture energy  $G_F$  for the bilinear case and expressing it by the softening parameter  $\beta$

$$G_F = \sigma_u w_u \left( \frac{1}{2} + \beta \left( \frac{w_c}{w_u} - 1 \right) \right) \quad (16)$$

the following expression is obtained for the brittleness number in the bilinear case

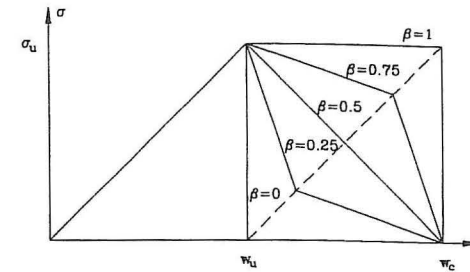


Figure 10. Definition of the softening parameter  $\beta$ .

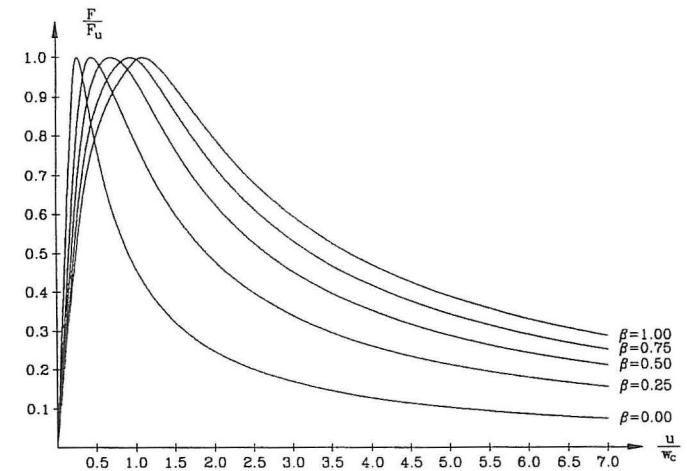


Figure 11. Influence of the shape of the softening relation described by the softening parameter  $\beta$ .

$$B = \frac{1}{\frac{1}{2} + \beta \left( \frac{w_c}{w_u} - 1 \right)} \quad (17)$$

The influence of  $\beta$  on the shape of the pull-out relation is illustrated in figure 11. In this case the force is normalised with the ultimate load  $F_u$  for each curve.

Size effects are studied by varying the size of the pull-out problem considering geometrically similar cases and comparing the ultimate load  $F_u$  normalised by  $\sigma_u L^2$ . The result is shown in figure 12. The maximum size effect that can be predicted by the model is found using the stress distributions  $\sigma = \sigma_u$  corresponding to ideal ductile behaviour (very small sizes) and  $\sigma = \sigma_u (R - r)/R$  corresponding to brittle behaviour (large sizes). Using these stress distributions in eq. (2) it is found that the maximum size effect predicted by the model is a factor of three -



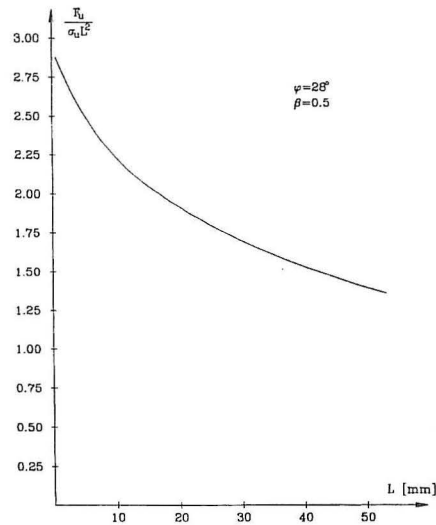


Figure 12. Model predicted size effects on the load-bearing capacity.

exactly the same as for a beam in bending, Ulfkjær et al. [17].

Note, that since the linear fracture mechanics is not incorporated in this model, no size effects are predicted when the size exceeds a certain level. This model predicts only the non-linear size effects, i.e. the size effects in the region where non-linear effects are dominating. In cases where the non-linear effects are not dominating, i.e. for very large specimens, using the results of the analysis carried out here might be misleading. However, the analysis indicates, figure 12, that for small embedment depths, for  $L$  ranging from 0 to about 50 mm, non-linear effects are dominating, and thus, the results predicted model should be representative.

### Calibration and evaluation

The bilinear model were calibrated on 18 pull-out tests in different sizes, the embedment length  $L$  ranging from 28 mm to 95 mm.

The calibration was performed by inspecting the fit visually using a computer programme allowing for easy adjustment of all relevant parameters. Figure 13 shows the result of a typical calibration. As it appears, the fit is quite good over the entire measurement range.

The parameters were calibrated in the following way. First, the stress  $\sigma_u$  was chosen as a fixed value close to the measured tensile strength of the concrete. Then the initial slope was calibrated as explained in the preceding section. Then the peak load and peak deformation were calibrated by simultaneously changing the radius  $R$  and the fracture energy  $G_F$ , and finally the shape was fine tuned by changing the softening parameter  $\beta$ .

The results of the calibrations are shown in table 1. As it appears, two values are given for the radius, the value  $R$  for the final radius observed after the test,

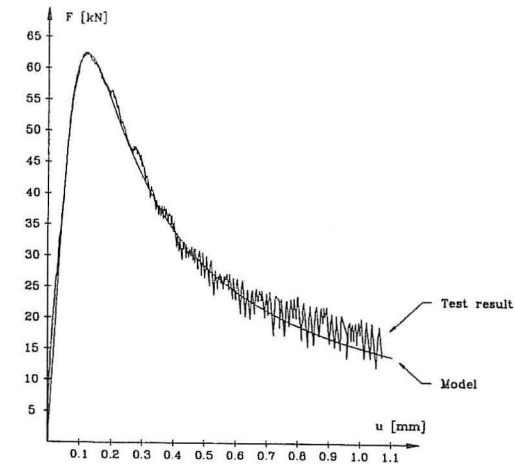


Figure 13. Calibration of model to test result.

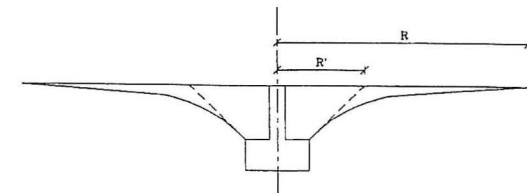


Figure 14. Radius  $R$  observed by test, and effective radius  $R'$  used in model.

and the effective radius  $R'$  as it was estimated by calibration of the model, figure 14. As it appears, typically there is a factor 2 – 3 between the two values. The results do not necessarily represent any serious discrepancy between the model and reality. The cones that were pulled off during the test showed a curved crack path corresponding to large initial values of  $\varphi$  that were substantially decreased during the fracture process. Thus, since the model include only one value of  $\varphi$ , and since this value should be close to the initial value of  $\varphi$  observed during the test, relatively small values of the radius  $R$  should be expected when calibrating the model.

Further, the values of the fracture energy estimated by the model, the effective fracture energy  $G'_F$ , is substantially larger than usual fracture energies for concrete. Since an ordinary high-strength concrete was used, this effect must be due to the model. However, as before, this is to be expected considering the low values of the effective radius  $R'$ . Since the area under the force-displacement curve is approximately correct, the following relationship between the real and the effective parameters must hold  $\pi R'^2 G'_F = \pi R^2 G_F$ . If the values of the effective fracture energy is interpreted in this way, the results become close to the values of the fracture energy usually observed experimentally.

An examination of the estimated values for the effective radius  $R'$  and for the



Name	L [mm]	R' [mm]	R [mm]	$\sigma_u$ [N/mm <sup>2</sup> ]	$w_u$ [mm]	$\sigma_b$ [N/mm <sup>2</sup> ]	$w_b$ [mm]	$G_F'$ [N/mm]	$\beta$	$\varphi$ [deg]
28-50-b	28	51	160	4.0	0.007	3.5	0.04	0.60	0.49	28.8
28-50-c	28	52	150	4.0	0.010	3.5	0.04	0.60	0.49	28.3
28-90-a	28	59	125	5.0	0.025	4.0	0.06	0.45	0.53	25.4
44-90-a	44	83	235	5.0	0.045	3.2	0.08	0.38	0.48	27.9
47-90-a	47	65	225	5.0	0.050	4.0	0.08	0.55	0.49	35.9
47-90-b	47	65	205	5.0	0.040	4.0	0.06	0.55	0.45	35.9
47-90-c	47	65	190	5.0	0.030	4.0	0.06	0.55	0.48	35.9
53-90-b	53	75	220	5.0	0.050	4.0	0.08	0.40	0.55	35.3
53-90-c	53	65	265	5.0	0.040	4.0	0.07	0.72	0.46	39.1
55-90-b	53	86	185	5.0	0.065	4.0	0.10	0.35	0.75	31.6
60-90-a	60	73	255	5.0	0.030	4.0	0.07	0.50	0.52	39.4
60-90-b	60	75	240	5.0	0.038	4.0	0.10	0.68	0.54	38.6
69-90-b	69	87	255	5.0	0.057	4.0	0.10	0.50	0.57	38.4
69-90-c	69	87	260	5.0	0.057	4.0	0.10	0.50	0.57	38.4
70-90-a	70	90	265	5.0	0.050	4.0	0.10	0.50	0.60	37.9
70-90-c	70	90	280	5.0	0.050	4.0	0.10	0.60	0.54	37.9
80-90-c	80	93	190	5.0	0.060	4.0	0.10	0.50	0.56	40.7
95-90-b	95	98	200	5.0	0.033	4.0	0.06	0.42	0.50	44.1

Table 1. Model parameters estimated by calibration of model.

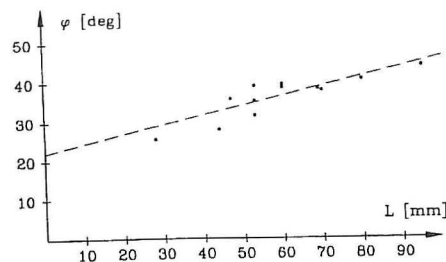


Figure 15. Estimated fracture angle  $\varphi$  as a function of the embedment depth.

initial angle  $\varphi$  indicates that the problem is not geometrically independent of the size. Figure 15 shows the estimated values of  $\varphi$  as a function of the size. As it appears, the fracture angle does not seem to be constant. The results indicate a typical value of  $\varphi$  around 20 – 25 degrees for very small embedment depths, and a value of  $\varphi$  around 40 degrees for embedment length around 100 mm.

As it appears, the softening parameter is in all cases very close to 0.5 corresponding to the single-linear case. Thus, the results indicate, that the improvement of the fit obtained by using a bilinear softening relation instead of the more simple single-linear softening relation is marginal.

## Conclusions

A simple model has been presented for the non-linear fracture mechanical problem of the pull-out of a concrete cone in a hook anchor failure test.

The model is formulated combining the fictitious crack model with very simple assumptions concerning the displacement field and the elastic response of the material around the crack path. Further, the solutions only correspond to an approximate satisfaction of the equilibrium equations.

Two models are formulated, one based on a single-linear softening relation, and one based on a bilinear softening relation. Both models define a simple brittleness number describing the shape of the pull-out relation.

The bilinear model was calibrated to 18 pull-out tests in different sizes. The model gave a fine fit to the experimentally measured pull-out curves, and the estimated model parameters correspond well to what should be expected. The results clearly indicate, that using this type of model, the gain in accuracy using a bilinear softening relation is marginal.

## References

- [1] Bocca, P., A. Carpinteri and S. Valente: *Fracture Mechanics Evaluation of Anchorage Bearing Capacity in Concrete*, Applications of Fracture Mechanics to Reinforced Concrete, Ed. A. Carpinteri, Elsevier Applied Science, 1990, pp. 231-265
- [2] Eligehausen, R. and G. Savade: *A Fracture Mechanics based Description of the Pull-Out Behaviour of Headed Studs Embedded in Concrete*, Ed. L. Elfgren, RILEM Report, Chapman and Hall, 1989, pp. 264-280.
- [3] Eligehausen, R. and Clausnitzer: *Analytisches Modell zur Beschreibung des Tragverhaltens von Befestigungselementen*, Report 4/1-83/3, Institut für Werkstoffe im Bauwesen, Universität Stuttgart.
- [4] Elfgren, L., U. Ohlson and K. Gylltoft: *Anchor Bolts Analysed with Fracture Mechanics*, Proc. of the International Conference on Concrete and Rock, Houston, Texas, June 17-19, 1987.
- [5] Rots, J.G.: *Simulation of Bond and Anchorage: Usefulness of Softening Fracture Mechanics*, Applications of Fracture Mechanics to Reinforced Concrete, Ed. A. Carpinteri, Elsevier Applied Science, 1990, pp. 231-265.
- [6] Elfgren, L., and U. Ohlson: *Anchor Bolts Modelled with Fracture Mechanics*, Applications of Fracture Mechanics to Reinforced Concrete, Ed. A. Carpinteri, Elsevier Applied Science, 1990, pp. 231-265.
- [7] Ozbolt, R. and Eligehausen: *Fastening Elements in Concrete Structures*, Fracture and Damage of Concrete and Rock, Ed. H.P. Rossmannith, Proc. of the 2nd International Conference on Fracture and Damage of Concrete and Rock, Vienna, Austria, E & FN Spon, 1993.
- [8] Tomasso, A.D., O. Manfrotti and G. Valente: *Comparison of Finite Element Concrete Models Simulating Pull-Out Tests*, Fracture and Damage of Concrete and Rock, Ed. H.P. Rossmannith, Proc. of the 2nd International Conference on Fracture and Damage of Concrete and Rock, Vienna, Austria, E & FN Spon, 1993.

- [9] Uchida, Y., K. Rokugo and W. Koyanagi: *Numerical Analysis of Anchor Bolts Embedded in Concrete Plates*, Fracture and Damage of Concrete and Rock, Ed. H.P. Rossmanith, Proc. of the 2nd International Conference on Fracture and Damage of Concrete and Rock, Vienna, Austria, E & FN Spon, 1993.
- [10] Hillerborg, A., M. Modeer and P.E. Petersson: *Analysis of Crack Formation and Crack Growth in Concrete by Means of Fracture Mechanics and Finite Elements*, Cement and Concrete Research, Vol. 6, No. 6, Nov. 1977.
- [11] Dugdale, D.S.: *Yielding of Steel Sheets Containing Slits*, Journal Mech. Phys. Solids, Vol. 8, 1960, pp. 100-104.
- [12] Barenblatt, G.I., in H.L. Dryden and T. Karman (eds.), pp. 56-131: *Advances in Applied Mechanics*, Academic, Vol. 7, 1962.
- [13] Hillerborg, A. and J.G. Rots: *Crack Concepts and Numerical Modelling* pp. 128-137 in L. Elfgren (ed.) *Fracture Mechanics of Concrete Structures*, Chapman and Hall, 1989.
- [14] Rots, J.G.: *Smearred Crack Approach*, in L. Elfgren (ed.) *Fracture Mechanics of Concrete Structures*, Chapman and Hall, pp. 138-146, 1989.
- [15] Petersson, P.E.: *Crack Growth and Development of Fracture Zones in Concrete and Similar Materials*, Report TVBM-1006, Division of Building Materials, Lund Institute of Technology, Sweden.
- [16] Brincker, R. and H. Dahl: *On the Fictitious Crack Model of Concrete Fracture*, Magazine of Concrete Research, Vol. 41, No. 147, pp. 79-86, June 1989.
- [17] Ulfkjær, J.P., S. Krenk and R. Brincker: *Analytical Model for Fictitious Crack Propagation in Concrete Beams*, Journal of Engineering Mechanics, Vol. 121, No. 1, January 1995.
- [18] Ulfkjær, J.P., O. Hededal, I. Kroon and R. Brincker: *Simple Applications of Fictitious Crack Model in Reinforced Concrete Beams*, Proc. of the IUTAM Symposium on Fracture of Brittle Disordered Materials, Concrete, Rock and Ceramics, Queensland, Australia, September 1993.
- [19] Ulfkjær, J.P., O. Hededal, I. Kroon and R. Brincker: *Simple Application of Fictitious Crack Model in Reinforced Concrete beams - Analysis and Experiment*, Proc. of the JCI International Workshop on size Effects in concrete Structures, Sendai, Japan, November 1993.
- [20] Bache, H.: *Brittleness/Ductility from a Deformation and Ductility points of View*, in L. Elfgren (ed.) *Fracture Mechanics of Concrete Structures*, Chapman and Hall, pp. 202-207, 1989.

## CONNECTIONS IN PRECAST BUILDINGS USING ULTRA HIGH-STRENGTH FIBRE REINFORCED CONCRETE

**Bjarne Chr. Jensen, Ph. D., director, professor**  
Carl Bro Group, Granskoven 8, DK-2600 Glostrup, Denmark

**Lars Rom Jensen, B.Sc., project manager**  
Carl Bro Group, Sohngaardsholmsvej 2, DK-9000 Aalborg, Denmark

**Lars Pilegaard Hansen, Ph. D., ass. professor**  
**Finn Toft Hansen, ass. professor**  
Aalborg University, Sohngaardsholmsvej 57, DK-9000 Aalborg, Denmark

### ABSTRACT

Precast elements have been used for decades in the building industry. Main reasons for this are reduction in price, reduction in erection time, and increase of the quality as production in factories often reduce the possibility of faults.

Since the beginning of the 70's, we have in Denmark made several attempts to change from large panel buildings into systems which allow much more flexibility in the use of the building including changes during the lifetime of the building. Column/beam/slab building systems have been introduced, but the flexibility is still limited.

Column/slab building systems are preferred, but due to transportation and lift capacities on the site, the size of the slab elements is limited.

A building system with great distance between columns, reasonable sizes of slab elements and great possibility for the architect to form the facades including use of balconies and chances in facade lines, would be a step forward for the building industry.

The Building Department of the Education Ministry has initiated such a development, and a very simple building systems will be used for the next building complex at Aalborg University.

The partners who did the development for the Building Department, are Carl Bro Group, Dall & Lindhardt and Aalborg University.

**Key Words:** Fibre reinforced concrete, joints, elements, ultimate load, fire resistance.